

BERNSTEIN NEURAL NETWORKS METHOD FOR SOLVING VARIABLE ORDER FRACTIONAL MIXED VOLTERRA-FREDHOLM INTEGRO-DIFFERENTIAL EQUATIONS

(Kaedah Rangkaian Neural Bernstein untuk Menyelesaikan Persamaan Kamir-Beza
Volterra-Fredholm Tercampur Pecahan Berperingkat Pembolehubah)

KAWTHAR ALSA'DI & NIK MOHD ASRI NIK LONG*

ABSTRACT

This paper deals with the drawback of the semi-group properties in variable order fractional mixed Volterra-Fredholm integro-differential equations (\mathcal{VO} -FVFIDEs) under Caputo derivative operator. The variable order of the equation is converted to piecewise constant functions by partition it into sub-intervals. The existence and uniqueness of solutions are investigated. A novel technique using Bernstein Neural Network (BernsteinNN) method is proposed to obtain the approximate solution for the FVFIDEs, which used the basis of Bernstein polynomials instead of the activation function in the artificial neural network method. The loss function is developed by adding the L_2 regularization for parameter terms and the hyper-parameter λ to ensure the stability of training process and to control the regularization strength, respectively. Adam optimization approach is applied to training the neural networks and the model performance is computed using the mean square error. The validity of the presented method is demonstrated through the presented example.

Keywords: fractional variable order; Caputo-fractional derivative; Bernstein neural network method; artificial neural network method; Adam optimization method

ABSTRAK

Kertas kerja ini membincangkan kekurangan sifat semi-kumpulan bagi persamaan kamir-beza Volterra-Fredholm tercampur pecahan berperingkat pembolehubah (FVFIDEs) di bawah pengoperasi pembeza Caputo. Peringkat pembolehubah bagi persamaan ditukarkan kepada fungsi pemalar cebis demi cebis dengan membahagikannya kepada sub-selang. Kewujudan dan keunikan penyelesaian disiasat. Suatu kaedah baharu menggunakan kaedah rangkaian neural Bernstein dicadangkan untuk mendapatkan penyelesaian hampiran bagi FVFIDEs, dengan menggunakan asas bagi polynomial Beinstein selain dari fungsi keaktifan di dalam kaedah rangkaian neural buatan. Fungsi terhilang dibina dengan menambah regularisasi L_2 bagi sebutan parameter dan hiper-parameter λ untuk memastikan kestabilan proses latihan dan mengawal kekuatan regularisasi, masing-masing. Kaedah pengoptimalan Adam digunakan untuk melatih rangkaian neural. Seterusnya, prestasi model dikira menggunakan ralat kuasa dua min. Keputusan berangka membuktikan keabsahan kaedah yang dicadangkan melalui contoh yang dibentangkan.

Kata kunci: pesanan berubah pecahan; terbitan pecahan Caputo; kaedah rangkaian neuron Bernstein; kaedah rangkaian neuron tiruan; kaedah pengoptimuman Adam

1. Introduction

Using variable-order (\mathcal{VO}) fractional operators instead of classical order is a powerful tool to understanding and interpreting non-linear mathematical models. They predict the behavior of these models in various scientific area, such as biology, disease modeling, chemistry, control system, and signal processing. Many recent studies have focused on investigating variable-order fractional differential equations (\mathcal{VO} -FDEs) within a theoretical framework, such as studying

the existence, uniqueness, and stability of solutions, and they refer to these concepts by the well-posedness analysis of the solution. For example, Rezapour *et al.* (2022) studied the fractional thermostat model with non-local boundary conditions, and presented the well-posedness analysis of solutions under the \mathcal{VO} -Caputo operator using fixed point theorem. Similarly, Van Bockstal *et al.* (2022) studied the existence and uniqueness for \mathcal{VO} -delay parabolic equations and used the Galerkin-Legendre spectral method and the backward Euler difference method to find the approximate solution. Moreover, Alharthi *et al.* (2023) investigated the existence and uniqueness of solutions for \mathcal{VO} -FDEs of fractal type and solved them numerically using linear interpolation and the Euler approximation. Ahmed *et al.* (2024) applied fixed-point theory to investigate the existence and uniqueness of chaotic dynamics in \mathcal{VO} -FDEs and compared the behavior of solutions using numerical simulations over a long time interval. Additionally, Yuan *et al.* (2023) analyzed the existence, uniqueness, and regularity of analytic solutions for linear \mathcal{VO} fractional diffusion equations and solved them using a piecewise polynomial collocation method.

Several studies have also focused on stability analysis. Darbo's fixed point theorem, Kuratowski measure of non-compactness, and Ulam-Hyers stability are used by Benkerrouche *et al.* (2022) to examine the well-posedness analysis of solutions for \mathcal{VO} -FDEs. Sarwar (2022) used continuation theorems to prove the global existence of solutions for \mathcal{VO} -FDEs and investigated different types of Ulam-Hyers stability. Awad *et al.* (2023) applied different fixed point theorems and Ulam-Hyers criterion to analyze the well-posedness of solutions for \mathcal{VO} -FDEs of φ -Caputo type. Furthermore, Albasheir *et al.* (2023) investigated the well-posedness analysis for \mathcal{VO} -FDEs. Xu *et al.* (2024) studied the existence and stability of solutions for RL-Atangana-Baleanu \mathcal{VO} -FDEs using Banach's and Krasnoselskii's fixed point theorems and examined their Ulam-Hyers stability. Benkerrouche *et al.* (2023) analyzed the existence and uniqueness of solutions for impulsive \mathcal{VO} -FDEs using Brouwer fixed point theorem and Banach contraction principle, while also investigating Ulam-Hyers stability. Bouazza *et al.* (2023a) examined the existence of solutions for Caputo-Hadamard \mathcal{VO} -FDEs and solved them using the upper-lower solution technique. Additionally, Derakhshan (2022) used Banach fixed point theorem and the contradiction method to study the existence and uniqueness of solutions for \mathcal{VO} -FDEs in fluid mechanics and demonstrated their Ulam-Hyers stability. They also proposed an operational matrix of shifted Legendre polynomials with collocation points to approximate solutions. Bouazza *et al.* (2023b) applied Darbo's fixed point theorem and Kuratowski's metric of non-compactness to investigate the existence of solutions for Riemann-Liouville \mathcal{VO} -FDEs and analyzed Ulam-Hyers-Rassias stability. Although the above studies utilized fixed-point theorems to explore theoretical aspects, some did not consider the limitations of the semi-group property for \mathcal{VO} -operators, which prevents the conversion of the equation into an integral form.

Various numerical methods have been applied to solve \mathcal{VO} -FDEs. For instance, Lagrange polynomial interpolation Kachia *et al.* (2020) used to solve different derivatives of \mathcal{VO} -FDEs with three-dimensional models for cancer growth evolution. Heydari & Atangana (2020) employed operational matrices of \mathcal{VO} -fractional generalized Lucas polynomials combined with Lagrange multipliers scheme at some collocation points to solve the \mathcal{VO} space-time mobile-immobile advection-dispersion equation. Zúñiga-Aguilar *et al.* (2017) applied the Levenberg-Marquardt algorithm with artificial neural networks to approximate the solutions of \mathcal{VO} -FDEs. Moghadam *et al.* (2020) used the Jacobi spectral collocation method to approximate the solution of the fractional advection-dispersion equation. Similarly, Babaei *et al.* (2020) employed the operational matrix of the sixth-kind Chebyshev collocation method to solve variable order fractional integro-differential equations (\mathcal{VO} -FIDEs). Tavares *et al.* (2016) approximated solutions for \mathcal{VO} -fractional partial differential equations by expressing three types of Caputo derivatives based on integer-order derivatives. Malesza *et al.* (2019) solved linear \mathcal{VO} -FDEs using a switching schemes approach and explored the duality properties between \mathcal{VO} -derivatives. Additionally, Zheng (2022) applied the collocation method to solve nonlinear \mathcal{VO} -FDEs under uniform and graded meshes. Cao & Qiu (2016) constructed a second-order approximation of the \mathcal{VO} -Riemann-Liouville fractional derivative and used it to approximate FDE solutions.

Moghaddam & Machado (2017) developed an explicit spline finite difference method to solve nonlinear diffusion \mathcal{VO} -FDEs. Li *et al.* (2017) approximated \mathcal{VO} -FDEs by converting them into an equivalent integer functional differential equation and solved using reproducing kernel method. Finally, Zuniga-Aguilar *et al.* (2019) applied Lagrange polynomial interpolation to solve both constant and \mathcal{VO} -Liouville-Caputo-type delay differential chaotic systems.

Limited studies have been published on variable-order fractional integro-differential equations (\mathcal{VO} -FIDEs). For example, Agarwal *et al.* (2021) employed operational matrices of shifted Vieta-Fibonacci polynomials to approximate the solutions of \mathcal{VO} -FIDEs. Ganji *et al.* (2020) utilized operational matrices of shifted Legendre polynomials combined with Newton-Cotes collocation points to solve \mathcal{VO} -FIDEs of Caputo type. Additionally, Alsa'di *et al.* (2024) conducted a comprehensive study investigating both the theoretical and approximate solutions for a mixed form of FVFIDEs with constant order, solving them using the Laplace Adomian decomposition method.

The semi-group property is a fundamental concept in solving differential equations and simplifying computations. It states that applying two consecutive operators is equivalent to applying a single operator with a combined order. For example, the Riemann-Liouville integral operator satisfies the semi-group property, such that $I^\alpha I^\beta \chi(s) = I^{\alpha+\beta} \chi(s)$. However, this property does not hold for \mathcal{VO} Riemann-Liouville and Caputo derivatives (i.e. $I^{\alpha(s)} D^{\beta(s)} \chi(s) \neq D^{\beta(s)-\alpha(s)} \chi(s)$) because they depend on initial conditions and historical (memory) data. Consequently, the fractional differential operator cannot be directly converted into its equivalent integral form.

In this study, we first extend the work in Alsa'di *et al.* (2024) to \mathcal{VO} equations. Then, by dividing the variable order into sub-intervals and expressing it as piecewise constant functions, we overcome the drawback associated with the semi-group properties. Next, we apply this technique to study the existence and uniqueness of the solution, following steps similar to those used for constant-order equations in Alsa'di *et al.* (2024). Finally, we solve the given equation using the newly developed method. Thus, we address the following FVFIDEs of the form:

$$\begin{aligned} {}^c D_{0+}^{\alpha(s)} \chi(s) &= \varphi(s) + \rho \int_0^s \int_0^C \mathcal{K}(x, v) \mathcal{H}(\chi(v)) dv dx, \\ \chi(0) &= \chi_0, \quad \chi'(0) = \chi_1, \end{aligned} \quad (1)$$

where ${}^c D^{\alpha(s)}$ is Caputo's fractional derivative with variable order $\alpha(s) \in (1, 2]$, $0 \leq s, x \leq C$, and $\rho > 0$ is a real constant. $\varphi : J = [0, C] \rightarrow \mathbb{R}$, the kernel $\mathcal{K}(x, v)$ and $\mathcal{H}(\chi(s))$ are continuous functions, $\chi(s)$ is an unknown function.

This paper is organized as follows. In Section 2, we recall some background of fractional calculus. In Section 3, we investigate the existence and uniqueness of the solution. Section 4 explained the developed method: Bernstein neural network. In Section 5, we present a numerical example. Finally, Section 6 is the conclusion.

2. Preliminary

In this section, we recall some basic concepts from fractional calculus and fixed-point theory in Banach space.

Let $\mathfrak{M} = \{\chi : \chi \in C(J)\}$ be the set of all continuous functions on the Banach space with the norm $\|\chi\| = \sup_{s \in J} |\chi(s)|$, and $J = [0, C]$. Let $AC^m(J)$ be the set of all continuously differentiable functions $\chi(u)$ on J .

Definition 2.1. (Kilbas *et al.* 2006) The Riemann-Liouville fractional integral of order $\alpha \in \mathbb{C}$

of a function $\chi(s)$ is given by

$$J_{a+}^{\alpha} \chi(s) = \frac{1}{\Gamma(\alpha)} \int_a^s (s-v)^{\alpha-1} \chi(v) dv, \quad (s > a; \Re(\alpha) > 0)$$

where Γ is Euler's Gamma function.

Definition 2.2. (Kilbas *et al.* 2006) The Caputo fractional derivative of order $\alpha \in \mathbb{C}$ of a continuous function $\chi(s)$ is defined by

$${}^c D_{a+}^{\alpha} \chi(s) = J_{a+}^{n-\alpha} \left(\frac{d^n}{ds^n} \chi(s) \right) = \frac{1}{\Gamma(n-\alpha)} \int_a^s (s-v)^{n-\alpha-1} \chi^{(n)}(v) dv, \quad s > a; \Re(\alpha) > 0$$

where $n = [\alpha] + 1$ and Γ is Euler's Gamma function.

These properties mentioned by (Kilbas *et al.* 2006) are important in our work: Let $\alpha > 0$ and $\gamma > 0$, and let $\chi \in L^1[a, b]$. Then

$$J_{a+}^{\alpha} J_{a+}^{\gamma} \chi(s) = J_{a+}^{\gamma} J_{a+}^{\alpha} \chi(s) = J_{a+}^{\alpha+\gamma} \chi(s), \quad (2)$$

$${}^c D_{a+}^{\alpha} [J_{a+}^{\alpha} \chi(s)] = \chi(s), \quad (3)$$

$$J_{a+}^{\alpha} [{}^c D_{a+}^{\alpha} \chi(s)] = \chi(s) - \sum_{k=0}^{n-1} \frac{\chi^{(k)}(a)}{k!} (s-a)^k \text{ for } n-1 < \alpha \leq n. \quad (4)$$

Moreover, If χ expressed as a power function, then the fractional integral given by:

Lemma 2.3. (Kilbas *et al.* 2006) If $\alpha \geq 0$ and $\gamma > 0$, then

$$J_{a+}^{\alpha} (s-a)^{\gamma-1} = \frac{\Gamma(\gamma)}{\Gamma(\gamma+\alpha)} (s-a)^{\gamma+\alpha-1} \quad (\alpha > 0),$$

$${}^c D_{a+}^{\alpha} (s-a)^{\gamma-1} = \frac{\Gamma(\gamma)}{\Gamma(\gamma-\alpha)} (s-a)^{\gamma-\alpha-1} \quad (\alpha \geq 0)$$

Definition 2.4. (Samko 1995) The Riemann-Liouville fractional integral of real order $\alpha(s) \in \mathbb{C}$ of a function $\chi(s)$ is given by

$$J_{a+}^{\alpha} \chi(s) = \frac{1}{\Gamma(\alpha(s))} \int_a^s (s-v)^{\alpha(s)-1} \chi(v) dv, \quad s > a; \Re(\alpha(s)) > 0$$

where Γ is Euler's Gamma function.

Definition 2.5. (Samko 1995) The Caputo fractional derivative of order $\alpha(s) \in \mathbb{C}$ of a continuous function $\chi(s)$ is defined by

$${}_0^C \mathcal{D}_x^{\alpha(s)} \chi(s) = \frac{1}{\Gamma(n-\alpha(s))} \int_0^s \frac{s^{(n)}(v) dv}{(s-v)^{\alpha(s)-n+1}}, \quad n-1 < \alpha(s) < n, \Re(\alpha(s)) > 0$$

where Γ represents Gamma function.

Definition 2.6. (Bhrawy and Zaky 2016) Let $\alpha(x)$ be the fractional order such that $\alpha(s) \in (1, 2]$. Then the following property hold

$${}_0^C \mathcal{D}_x^{\alpha(s)} s^{\gamma} = \begin{cases} 0, & \gamma = 0, 1, \\ \frac{\Gamma(\gamma+1)}{\Gamma(\gamma+1-\alpha(s))} s^{\gamma-\alpha(s)}, & \gamma = 2, 3, \dots \end{cases}$$

Definition 2.7. (equicontinuous function) (Kilbas 2001) A set $G = \chi_n$ is called equicontinuous if $\forall \epsilon > 0, \exists \delta > 0$ such that, for all $\forall \chi \in G$ and $\forall s_1, s_2 \in [a, b], |s_1 - s_2| < \delta$, we have $|\chi(s_1) - \chi(s_2)| < \epsilon$.

Theorem 2.8. (Arzelà-Ascoli theorem) (Zhou et al. 2016) "If a family $\chi = \{\chi(s)\}$ in $C(J, \mathbb{R})$ is uniformly bounded and equicontinuous on J , and for any $s^* \in J, \{\chi(s^*)\}$ is relatively compact, then χ has a uniformly convergent subsequence $\{\chi_n(s)\}_{n=1}^\infty$ ".

As a result of Theorem 2.8: "A set $\chi \in C(J, \mathbb{R})$ is consider relatively compact when it satisfies both uniform boundedness and equicontinuity over the interval J " (Zhou et al. 2016).

Theorem 2.9. (Banach Contraction Principle) (Zhou et al. 2016) Let (X, d) be a complete metric space, and $\chi : X \rightarrow X$ a contraction mapping. Then, there exists a unique fixed point s of χ in X , i.e., $\chi s = s$.

Theorem 2.10. (Schaefer's fixed point theorem) (Zhou 2023) Let $\chi : X \rightarrow X$ be a completely continuous operator. If the set $E(\chi) = \{u \in X : u = \tau \chi u \text{ for some } \tau \in [0, 1]\}$ is bounded, then, χ has a fixed point.

3. Theoretical results

This section examine the existence and uniqueness of solution for \mathcal{VO} -FVFIDEs. We need the following axioms:

(A1) Let $\mathcal{H}, \mathcal{K}(x, v)$ and φ are continuous functions, such that \mathcal{H} satisfies the Liptchiz condition: $||\mathcal{H}(x) - \mathcal{H}(y)|| \leq L||x - y||, \forall x, y \in \mathbb{R}$, with Liptchiz constant $L > 0$, $\mathcal{K}^* = \sup_{x,v \in J} \mathcal{K}(x, v) = ||\mathcal{K}(x, v)||$, and continuity bounded function φ satisfies $\sup_{s \in J} |\varphi(s)| = ||\varphi(s)||$.

(A2) Let \mathcal{H} be bounded function on Banach space, such that $\forall s \in J, \chi \in \mathbb{R}, \exists z > 0$, such that $||\mathcal{H}(\chi(s))|| \leq z ||\chi||$.

(A3) Let $\{s_k\}_{k=0}^n$ be the finite sequence of points such that $0 = s_0 < s_k < s_n = C, k = 1, \dots, n-1$ where $\mathcal{J} = \bigcup_{k=1}^n J_k$ is a partition of $[0, C]$ with $J_k := (s_{k-1}, s_k], k = 1, 2, \dots, n$, for $n \in \mathbb{N}$. Let the variable order $\alpha(s) : [0, C] \rightarrow (1, 2]$ be a piece-wise constant function with respect to \mathcal{J} , defined by $\alpha(s) = \sum_{k=1}^n \alpha_k I_k(s)$, where $\alpha_k \in (1, 2], k = 1, 2, \dots, n$ are constants, and $I_k(s)$ is the indicator of the interval $(s_{k-1}, s_k]$ and defined by

$$I_k(s) = \begin{cases} 1, & \text{for } s \in J_k \\ 0, & \text{elsewhere.} \end{cases} \quad (5)$$

By using Eq. 5 as mentioned in Axiom (A3), the \mathcal{VO} -Caputo derivative with order $\alpha(s) \in (1, 2]$ in Eq. (1) can be expressed as

$$\begin{aligned} {}^c D_{0+}^{\alpha(s)} \chi(s) &= \int_0^s \frac{(s-v)^{1-\alpha(s)}}{\Gamma(2-\alpha(s))} \chi''(v) dv, \\ &= \int_0^s I_1(s) \frac{(s-v)^{1-\alpha_1}}{\Gamma(2-\alpha_1)} \chi''(v) dv + \dots + \int_0^s I_k(s) \frac{(s-v)^{1-\alpha_k}}{\Gamma(2-\alpha_k)} \chi''(v) dv \quad (6) \\ &= \sum_{k=1}^n I_k(s) \int_0^s \frac{(s-v)^{1-\alpha_j}}{\Gamma(2-\alpha_j)} \chi''(v) dv. \end{aligned}$$

Equation (6) explains how the Caputo derivative can be written as a partition of the variable order $\alpha(s)$ as a piecewise constant function. This construction leads to a better understanding of function's behavior across different parts. Additionally, it is easy to implement the semi-group property on each partition.

Hence, Eq. (1) can be re-written as

$$\sum_{k=1}^n \int_{s_{k-1}}^{\min(s, s_k)} \frac{(s-v)^{1-\alpha_k}}{\Gamma(2-\alpha_k)} \chi''(v) dv = \varphi(s) + \rho \sum_{k=1}^n \int_{s_{k-1}}^{\min(s, s_k)} \int_0^C \mathcal{K}(x, v) \mathcal{H}(\chi(v)) dv dx, \quad (7)$$

with initial conditions $\chi(0) = \chi_0$, $\chi'(0) = \chi_1$.

Suppose that $s = \min(s, s_k)$ on sub-interval $[s_{k-1}, s_k]$, it is sufficient to prove the existence and uniqueness of this partition with constant fractional order as

$$\int_{s_{k-1}}^s \frac{(s-v)^{1-\alpha_k}}{\Gamma(2-\alpha_k)} \chi''(v) dv = \varphi(s) + \rho \int_{s_{k-1}}^s \int_0^C \mathcal{K}(x, v) \mathcal{H}(\chi(v)) dv dx, \quad (8)$$

which exactly satisfy the constant FVFIDEs of the form

$${}^c D_{s_{k-1}^+}^{\alpha_k} \chi(s) = \varphi(s) + \rho \int_{s_{k-1}}^s \int_0^C \mathcal{K}(x, v) \mathcal{H}(\chi(v)) dv dx, \quad s \in J_k \quad (9)$$

with initial condition $\chi(s_{k-1}) = \chi_0$, $\chi'(s_{k-1}) = \chi_1$.

Lemma 3.1. *Let Axioms (A1)–(A3) hold. Let $\chi \in \mathfrak{M}$, and $s \in J$. The solution χ satisfies Eq. (9) if and only if χ satisfies the integral equation*

$$\begin{aligned} \chi(s) = & \chi_0 + \chi_1(s - s_{k-1}) + \frac{1}{\Gamma(\alpha)} \int_{s_{k-1}}^s (s - \omega)^{\alpha-1} \varphi(\omega) d\omega \\ & + \frac{\rho}{\Gamma(\alpha)} \int_{s_{k-1}}^s (s - \omega)^{\alpha-1} \left(\int_{s_{k-1}}^{\omega} \int_0^C \mathcal{K}(x, r) \mathcal{H}(\chi(r)) dr dx \right) d\omega. \end{aligned} \quad (10)$$

Proof. Applying the integral $I_{s_{k-1}^+}^{\alpha_k}$ of order α_k mentioned in Definition 2.4 to Eq. (9) gives

$$J_{s_{k-1}^+}^{\alpha_k} ({}^c D_{s_{k-1}^+}^{\alpha_k} \chi(s)) = J_{s_{k-1}^+}^{\alpha_k} (\varphi(s)) + \rho J_{s_{k-1}^+}^{\alpha_k} \left(\int_{s_{k-1}}^s \int_0^C \mathcal{K}(x, v) \mathcal{H}(\chi(v)) dv dx \right). \quad (11)$$

Using the fractional property Eq. (4) in Eq. (11) with $a = s_{k-1}$ and $n = 2$, we obtain

$$\chi(s) = \chi(s_{k-1}) + \chi'(s_{k-1})(s - s_{k-1}) + J_{s_{k-1}^+}^{\alpha_k} (\varphi(s)) + \rho J_{s_{k-1}^+}^{\alpha_k} \left(\int_{s_{k-1}}^s \int_0^C \mathcal{K}(x, v) \mathcal{H}(\chi(v)) dv dx \right). \quad (12)$$

Substitute the initial conditions $\chi(s_{k-1}) = \chi_0$ and $\chi'(s_{k-1}) = \chi_1$ in Eq. (12), we obtain the result in Eq. (10).

To prove the converse, suppose that the integral in Eq. (10) is given. Apply the Caputo

fractional derivative ${}^c D_{0+}^{\alpha_k}$ of order $1 < \alpha_k \leq 2$ to both side of Eq. (10), then we have

$$\begin{aligned} & {}^c D_{0+}^{\alpha_k} \left(\chi(s) - \chi_0 - \chi_1(s - s_{k-1}) \right) \\ &= {}^c D_{0+}^{\alpha_k} \left(J_{0+}^{\alpha_k}(\varphi(s)) \right) + \rho {}^c D_{0+}^{\alpha_k} \left(J_{0+}^{\alpha} \left(\int_{s_{k-1}}^s \int_0^C \mathcal{K}(x, v) \mathcal{H}(\chi(v)) dv dx \right) \right). \end{aligned} \quad (13)$$

Using the properties in Eq. (3) and Lemma 2.3, then substitute the initial conditions into Eq. (13), we obtain Eq. (9). The proof is complete. \square

Note that the following results are valid in all scenarios, that the Eq. (9) is formulated based on the construction of Eq. (7), and hence Eq. (1) holds.

To prove our main results, we need to transform Eq. (9) to the fixed point problem, for this purpose, we define the operator $\Omega_\chi : \mathfrak{M} \rightarrow \mathfrak{M}$ as

$$\begin{aligned} \Omega_\chi(s) = & \chi_0 + \chi_1(s - s_{k-1}) + \frac{1}{\Gamma(\alpha_k)} \int_{s_{k-1}}^s (s - \omega)^{\alpha_k-1} \varphi(\omega) d\omega \\ & + \frac{\rho}{\Gamma(\alpha_k)} \int_{s_{k-1}}^s (s - \omega)^{\alpha_k-1} \left(\int_{s_{k-1}}^\omega \int_0^C \mathcal{K}(x, r) \mathcal{H}(\chi(r)) dr dx \right) d\omega. \end{aligned} \quad (14)$$

Then, Theorem 2.10 and Theorem 2.8 can be used to investigate the existence of the solution in next theorem.

Theorem 3.2. *Suppose that Axioms (A1) - (A3) hold, and consider the operator Ω_χ defined in Eq. (14). Then, Eq. (9) has at least one solution on J . Consequently, Eq. (7) also has at least one solution.*

Proof. To prove the existence of the solution, we present the proof in the following steps. To show that Ω_χ is completely continuous:

Step 1: Need to show that Ω_χ is continuous. Let $\{\chi_n\}$ be a sequence such that $\chi_n \rightarrow \chi$ in \mathfrak{M} . Then for each $s \in J$, we have

$$\begin{aligned} & \|\Omega_{\chi_n}(s) - \Omega_\chi(s)\| \\ & \leq \frac{\rho}{\Gamma(\alpha_k)} \int_{s_{k-1}}^s (s - \omega)^{\alpha_k-1} \left(\int_{s_{k-1}}^\omega \int_0^C |\mathcal{K}(x, r)| \|\mathcal{H}(\chi_n(r)) - \mathcal{H}(\chi(r))\| dr dx \right) d\omega \\ & \leq \frac{\rho L}{\Gamma(\alpha_k)} \int_0^s (s - \omega)^{\alpha_k-1} \left(\int_{s_{k-1}}^\omega \int_0^C \sup_{s \in J} |\mathcal{K}(x, r)| \|\chi_n(s) - \chi(s)\| dr dx \right) d\omega. \end{aligned}$$

By using the hypotheses in (A1), we have

$$\begin{aligned} \|\Omega_{\chi_n}(s) - \Omega_\chi(s)\| & \leq \frac{\rho L \mathcal{K}^*}{\Gamma(\alpha)} \|\chi_n(s) - \chi(s)\| \int_0^s (s - \omega)^{\alpha-1} \left(\int_0^\omega \int_0^C dr dx \right) d\omega \\ & \leq \frac{\rho L \mathcal{K}^* C^{\alpha+2}}{\Gamma(\alpha + 2)} \|\chi_n(s) - \chi(s)\|. \end{aligned}$$

Since the length of the uniformly partition of the sub-intervals $\sum_{k=1}^n [s_{k-1}, s_k]$ is the length of

$[0, C]$, take

$$\frac{\rho L \mathcal{K}^* C (s_k - s_{k-1})^{\alpha_k+1}}{\Gamma(\alpha_k + 2)} \leq \frac{\rho L \mathcal{K}^* C^{\alpha_k+2}}{\Gamma(\alpha_k + 2)} =: \mathcal{R} \quad (15)$$

Then $\|\Omega_{\chi_n}(s) - \Omega_\chi(s)\| \leq \mathcal{R} \|\chi_n(s) - \chi(s)\|$. As n approaches to infinity and $\chi_n \rightarrow \chi$, we obtain $\|\Omega_{\chi_n}(s) - \Omega_\chi(s)\| \rightarrow 0$. Hence, the continuity of operator Ω_χ is hold.

Step 2: Need to show the operator Ω_χ is uniformly bounded on \mathfrak{M} on each sub-interval on our partition. It sufficient to demonstrate that for $\varepsilon > 0$, $\exists Q > 0$, such that $\forall \chi \in B_\varepsilon =: Nb(\varepsilon) = \{\chi \in \mathfrak{M} : \|\chi\| \leq \varepsilon\}$, $\|\Omega_\chi(s)\| \leq Q$. To clarify this, let $\chi \in B_\varepsilon$ and for all $s \in J$, take the supremum norm for Ω , we obtain

$$\begin{aligned} \|\Omega_\chi(s)\| &\leq |\chi_0 + \chi_1(s - s_{k-1})| + \frac{1}{\Gamma(\alpha_k)} \int_{s_{k-1}}^s (s - \omega)^{\alpha_k-1} \sup_{\omega \in J} |\varphi(\omega)| d\omega \\ &\quad + \frac{\rho}{\Gamma(\alpha_k)} \int_{s_{k-1}}^s (s - \omega)^{\alpha_k-1} \left(\int_{s_{k-1}}^\omega \int_0^C \sup_{x, r \in J} |\mathcal{K}(x, r)| \sup_{r \in J} |\mathcal{H}(\chi(r))| dr dx \right) d\omega. \end{aligned}$$

Using the hypotheses in (A1), with few computations for the integral terms, by letting $t = s - \omega$ and change the limit of integration, we obtain

$$\|\Omega_\chi(s)\| \leq \|\chi_0\| + \|\chi_1\| C + \frac{C^{\alpha_k}}{\alpha_k \Gamma(\alpha_k)} \|\varphi(s)\| + \frac{\rho C^{\alpha_k+2} \mathcal{K}^*}{\alpha_k (\alpha_k + 1) \Gamma(\alpha_k)} \|\mathcal{H}(\chi(s))\|.$$

By using the boundedness of χ in (A2), we have

$$\begin{aligned} \|\Omega_\chi(s)\| &\leq \|\chi_0\| + \|\chi_1\| C + \frac{C^{\alpha_k}}{\Gamma(\alpha_k + 1)} \|\varphi(s)\| + \frac{\rho C^{\alpha_k+2} \mathcal{K}^*}{\Gamma(\alpha_k + 2)} z \|\chi\| \\ &\leq \|\chi_0\| + \|\chi_1\| C + \frac{C^{\alpha_k}}{\Gamma(\alpha_k + 1)} \|\varphi(s)\| + \frac{\rho C^{\alpha_k+2} \mathcal{K}^*}{\Gamma(\alpha_k + 2)} z \varepsilon. \end{aligned} \quad (16)$$

Define the constant $Q > 0$, such as

$$Q := \|\chi_0\| + \|\chi_1\| C + \frac{C^{\alpha_k}}{\Gamma(\alpha_k + 1)} \|\varphi(s)\| + \frac{\rho C^{\alpha_k+2} \mathcal{K}^*}{\Gamma(\alpha_k + 2)} z \varepsilon. \quad (17)$$

Then $\|\Omega_\chi(s)\| \leq Q$. Hence, the operator Ω_χ is uniformly bounded.

Step 3: To show that Ω_χ is equicontinuous. Assume that $s_k, s_{k^*} \in J$ such that $s_{k-1} < s_k < s_{k^*}$, then

$$\begin{aligned} &\|\Omega_\chi(s_{k^*}) - \Omega_\chi(s_k)\| \\ &\leq \|\chi_1(s_{k^*} - s_k)\| + \frac{1}{\Gamma(\alpha_k)} \int_{s_{k-1}}^{s_{k^*}} (s_{k^*} - \omega)^{\alpha_k-1} \|\varphi(s)\| d\omega \\ &\quad - \frac{1}{\Gamma(\alpha_k)} \int_{s_{k-1}}^{s_k} (s_k - \omega)^{\alpha_k-1} \|\varphi(s)\| d\omega \\ &\quad + \frac{\rho}{\Gamma(\alpha_k)} \int_{s_{k-1}}^{s_{k^*}} (s_{k^*} - \omega)^{\alpha_k-1} \left(\int_{s_{k-1}}^\omega \int_0^C \|\mathcal{K}(x, r)\| \|\mathcal{H}(\chi(r))\| dr dx \right) d\omega \\ &\quad - \frac{\rho}{\Gamma(\alpha_k)} \int_{s_{k-1}}^{s_k} (s_k - \omega)^{\alpha_k-1} \left(\int_{s_{k-1}}^\omega \int_0^C \|\mathcal{K}(x, r)\| \|\mathcal{H}(\chi(r))\| dr dx \right) d\omega. \end{aligned}$$

Adding the integral terms $\pm \int_{s_{k-1}}^{s_k} (s_{k^*} - \omega)^{\alpha_k-1}$ for the previous step as follows:

$$\begin{aligned}
 & \|\Omega_\chi(s_{k^*}) - \Omega_\chi(s_k)\| \\
 & \leq \|\chi_1(s_{k^*} - s_k)\| + \frac{1}{\Gamma(\alpha_k)} \int_{s_{k-1}}^{s_{k^*}} (s_{k^*} - \omega)^{\alpha_k-1} \|\varphi(s)\| d\omega \\
 & \quad - \frac{1}{\Gamma(\alpha_k)} \int_{s_{k-1}}^{s_k} (s_{k^*} - \omega)^{\alpha_k-1} \|\varphi(s)\| d\omega + \frac{1}{\Gamma(\alpha_k)} \int_{s_{k-1}}^{s_k} (s_{k^*} - \omega)^{\alpha_k-1} \|\varphi(s)\| d\omega \\
 & \quad - \frac{1}{\Gamma(\alpha_k)} \int_{s_{k-1}}^{s_k} (s_k - \omega)^{\alpha_k-1} \|\varphi(s)\| d\omega \\
 & \quad + \frac{\rho}{\Gamma(\alpha_k)} \int_{s_{k-1}}^{s_{k^*}} (s_{k^*} - \omega)^{\alpha_k-1} \left(\int_{s_{k-1}}^\omega \int_0^C \|\mathcal{K}(x, r)\| \|\mathcal{H}(\chi(r))\| dr dx \right) d\omega \\
 & \quad - \frac{\rho}{\Gamma(\alpha_k)} \int_{s_{k-1}}^{s_k} (s_{k^*} - \omega)^{\alpha_k-1} \left(\int_{s_{k-1}}^\omega \int_0^C \|\mathcal{K}(x, r)\| \|\mathcal{H}(\chi(r))\| dr dx \right) d\omega \\
 & \quad + \frac{\rho}{\Gamma(\alpha_k)} \int_{s_{k-1}}^{s_k} (s_{k^*} - \omega)^{\alpha_k-1} \left(\int_{s_{k-1}}^\omega \int_0^C \|\mathcal{K}(x, r)\| \|\mathcal{H}(\chi(r))\| dr dx \right) d\omega \\
 & \quad - \frac{\rho}{\Gamma(\alpha_k)} \int_{s_{k-1}}^{s_k} (s_k - \omega)^{\alpha_k-1} \left(\int_{s_{k-1}}^\omega \int_0^C \|\mathcal{K}(x, r)\| \|\mathcal{H}(\chi(r))\| dr dx \right) d\omega.
 \end{aligned}$$

Gathering some terms in the previous inequality, we have

$$\begin{aligned}
 & \|\Omega_\chi(s_{k^*}) - \Omega_\chi(s_k)\| \\
 & \leq \|\chi_1(s_{k^*} - s_k)\| + \frac{1}{\Gamma(\alpha_k)} \int_{s_k}^{s_{k^*}} (s_{k^*} - \omega)^{\alpha_k-1} \|\varphi(w)\| dw \\
 & \quad + \frac{1}{\Gamma(\alpha_k)} \int_{s_{k-1}}^{s_k} ((s_{k^*} - \omega)^{\alpha_k-1} - (s_k - \omega)^{\alpha_k-1}) \|\varphi(w)\| dw \\
 & \quad + \frac{\rho}{\Gamma(\alpha_k)} \int_{s_k}^{s_{k^*}} (s_{k^*} - \omega)^{\alpha_k-1} \left(\int_{s_{k-1}}^\omega \int_0^C \|\mathcal{K}(x, r)\| \|\mathcal{H}(\chi(r))\| dr dx \right) d\omega \\
 & \quad + \frac{\rho}{\Gamma(\alpha_k)} \int_{s_{k-1}}^{s_k} ((s_{k^*} - \omega)^{\alpha_k-1} - (s_k - \omega)^{\alpha_k-1}) \left(\int_{s_{k-1}}^\omega \int_0^C \|\mathcal{K}(x, r)\| \|\mathcal{H}(\chi(r))\| dr dx \right) d\omega.
 \end{aligned}$$

Applying the hypotheses in (A1), then computing the integral as in Step 2, we obtain

$$\begin{aligned}
 & \|\Omega_\chi(s_{k^*}) - \Omega_\chi(s_k)\| \\
 & \leq \|\chi_1\| (s_{k^*} - s_k) + \frac{(s_{k^*} - s_{k-1})^{\alpha_k} + (s_k - s_{k-1})^{\alpha_k}}{\Gamma(\alpha_k + 1)} \|\varphi(s)\| \\
 & \quad + \frac{(s_{k^*} - s_{k-1})^{\alpha_k} + (s_k - s_{k-1})^{\alpha_k}}{\Gamma(\alpha_k + 1)} \rho \mathcal{K}^*_{\mathcal{Z}} \varepsilon.
 \end{aligned}$$

Hence, by using Definition 2.7, $\|\Omega_\chi(s_{k^*}) - \Omega_\chi(s_k)\| \rightarrow 0$ as $s_{k^*} \rightarrow s_k$, which means all χ_n behave uniformly with respect to continuity, and hence the operator Ω_χ is equicontinuous.

From Steps 1-3 and Theorem 2.8, we deduce that Ω_χ is a completely continuous operator. Next step, we will prove that Ω_χ is bounded set.

Step 4: To show that $\mathcal{U} = \{\chi \in \mathfrak{M} : \chi = \delta_k \Omega_\chi, \delta_k \in (0, 1)\}$ is a bounded set in \mathfrak{M} . Let

$\chi \in \mathcal{U}$, then $\chi = \delta_k \Omega_\chi$, for some $\delta \in (0, 1)$. Thus, for each $s \in J$, we have

$$\begin{aligned} \chi(s) = & \delta_k (\chi_0 + \chi_1(s - s_{k-1})) + \frac{\delta_k}{\Gamma(\alpha_k)} \int_{s_{k-1}}^s (s - \omega)^{\alpha_k-1} \varphi(\omega) d\omega \\ & + \frac{\rho \delta_k}{\Gamma(\alpha_k)} \int_{s_{k-1}}^s (s - \omega)^{\alpha_k-1} \left(\int_{s_{k-1}}^\omega \int_0^C \mathcal{K}(x, r) \mathcal{H}(\chi(r)) dr dx \right) d\omega. \end{aligned}$$

By using the boundedness property of $\|\Omega_\chi\|$ as in Step 2 with $\delta_k \in (0, 1)$ and applying the norm, we obtain

$$\|\chi(s)\| = \|\delta_k \Omega_\chi\| = \|\delta_k\| \|\Omega_\chi\| < \|\Omega_\chi\| \leq Q,$$

where Q is defined in Eq.(17). Thus, $\|\chi(s)\| \leq Q$, which prove that \mathcal{U} is bounded.

Combining all result above with Step 4, and using Theorem 2.10, we conclude that Ω_χ has a fixed point which is a solution of Eq. (9), and hence, the solution of Eq. (7) exists. \square

Theorem 3.3. Suppose that Axioms (A1) - (A3) hold. Eq. (9) has a unique solution on J (and consequently, Eq. (7) also has at least one solution), if there exist a constant \mathcal{R} satisfies $\mathcal{R} = \left(\frac{\rho L \mathcal{K}^* C^{\alpha_k+2}}{\Gamma(\alpha_k + 2)} \right) < 1$.

Proof. For $s \in J$ and $\mathcal{U}, \mathcal{V} \in \mathfrak{M}$, we have

$$\begin{aligned} & \|\Omega_{\mathcal{U}}(s) - \Omega_{\mathcal{V}}(s)\| \\ & \leq \frac{\rho}{\Gamma(\alpha_k)} \int_{s_{k-1}}^s (s - \omega)^{\alpha_k-1} \left\| \int_{s_{k-1}}^\omega \int_0^C \mathcal{K}(x, r) [\mathcal{H}(\mathcal{U}(r)) - \mathcal{H}(\mathcal{V}(r))] dr dx \right\| d\omega. \end{aligned}$$

Applying hypotheses in (A1) for \mathcal{H} and the kernel $\mathcal{K}(x, r)$, then integrate we have

$$\begin{aligned} \|\Omega_{\mathcal{U}}(s) - \Omega_{\mathcal{V}}(s)\| & \leq \frac{\rho L}{\Gamma(\alpha_k)} \int_{s_{k-1}}^s (s - \omega)^{\alpha_k-1} \left(\int_{s_{k-1}}^\omega \int_0^C \|\mathcal{K}(x, r)\| \|\mathcal{U}(r) - \mathcal{V}(r)\| dr dx \right) d\omega \\ & \leq \frac{\rho L \mathcal{K}^*}{\Gamma(\alpha_k)} \left(\int_{s_{k-1}}^s (s - \omega)^{\alpha_k-1} \int_{s_{k-1}}^\omega \int_0^C dr dx d\omega \right) \|\mathcal{U}(s) - \mathcal{V}(s)\| \\ & \leq \frac{\rho L \mathcal{K}^* C^{\alpha_k+2}}{\Gamma(\alpha_k + 2)} \|\mathcal{U}(s) - \mathcal{V}(s)\| \\ & \leq \mathcal{R} \|\mathcal{U}(s) - \mathcal{V}(s)\|. \end{aligned}$$

Since $\mathcal{R} < 1$, we conclude that Ω_χ is a contraction. Using Theorem 2.9, we confirm that Ω has a unique fixed point which is a solution of Eq. (9), and hence Eq. (7) has a unique fixed point. \square

4. Bernstein neural network method

In this section, we develop the Bernstein Neural Network (BernsteinNN) method for solving \mathcal{VO} FVFIDEs. The motivation for using Bernstein polynomials lies in their ability to provide accurate approximations for smooth and continuous functions, particularly fractional integro-differential equations. Additionally, Bernstein polynomials are numerically stable and exhibit less oscillation compared to other polynomial bases, such as Chebyshev or Legendre polyno-

mials, making them a robust choice for neural network-based approximations. They also offer straightforward computation, especially when integrated with neural networks.

Traditional numerical methods require discretization and often suffer from high computational complexity when dealing with fractional-order problems. In contrast, neural networks provide an alternative approach that can generalize solutions across different fractional operators without requiring explicit discretization. Thus, combining neural networks with Bernstein polynomials leverages the strengths of both approaches, ensuring stability in the approximate solution while achieving high accuracy with lower computational cost. Moreover, the flexibility of neural networks enables them to effectively approximate nonlinearities, making them well-suited for solving complex fractional integro-differential equations.

BernsteinNN is a simple neural network that uses Bernstein polynomial basis functions $B_n(s)$ instead of an activation function. This network consists of a single hidden layer, where the basis functions are combined into one layer, and the output is generated as a linear combination of these basis functions without using an activation function.

4.1. Construct the Bernstein neural network solution

Let us recall the general formulas for the Bernstein polynomial.

$$B_{j,n}(s) = C_n^j s^j (1-s)^{n-j}, \quad j = 0, 1, \dots, n, \quad (18)$$

Depends on the general form of the polynomial neural network which is mentioned above, use Bernstein polynomial $B_n(s)$ instead of $P_n(s)$. Hence, the general trial neural network solution $\hat{\chi}(s, B_n(s))$ with input s and polynomial $B_n(s)$ can be expressed as

$$\hat{\chi}(s, B_n(s)) = \sigma(s) + \phi(s, N(s, B_n(s))), \quad (19)$$

where the first part $\sigma(s)$ satisfies only initial/boundary conditions, and the second part $\phi(s, N(s, B_n(s)))$ contains single output $N(s, B_n(s))$ of BernsteinNN with input s and $B_n(s)$ and expressed as

$$N(s, B_n(s)) = \sum_{j=1}^n w_j B_{j-1}(s), \quad (20)$$

with $j = \{1, 2, 3, \dots, m\}$. Here, $N(s, B_n(s))$ consists of Bernstein polynomials, which are flexible in approximating smooth functions.

Now, let us derive the trial solution corresponding to our equation. To construct $\sigma(s)$ such that it satisfies the given initial conditions, write $\sigma(s)$ as

$$\sigma(s) = \chi_0 + \chi_1 s. \quad (21)$$

To check for the initial conditions, at $s = 0$:

$$\sigma(0) = \chi_0 + \chi_1(0) = \chi_0,$$

which satisfies $\chi(0) = \chi_0$. To check for the second condition, derivative $\sigma(s)$

$$\sigma'(s) = \chi_1,$$

and at $s = 0$:

$$\sigma'(0) = \chi_1,$$

which satisfies $\vartheta'(0) = \chi_1$. Thus, the function $\sigma(s) = \chi_0 + \chi_1 s$ is a valid choice. So, the final

trial solution for Eq. (21) will be written as

$$\hat{\chi}(s, B_n(s)) = \chi_0 + \chi_1 s + \phi(s, N(s, B_n(s))). \quad (22)$$

To ensure that the trial solution in Eq. (22) satisfies the initial conditions exactly, we define:

$$\phi(s, N(s, B_n(s))) = s^2 N(s, B_n(s)), \quad (23)$$

where s^2 is the multiplicative term to guarantee that $\phi(s, N(s, B_n(s)))$ vanishes at $s = 0$, preserving the initial conditions imposed by $\sigma(s)$, and $N(s, B_n(s))$ is the output of the Bernstein Neural Network, which takes the form in Eq. (20).

Note that, at $s = 0$, we require $\phi(0, N(0, B_n(0))) = 0$, ensuring:

$$\hat{\chi}(0, B_n(0)) = \sigma(0) + \phi(0, N(0, B_n(0))) = \chi_0 + 0 = \chi_0.$$

Then, compute the first derivative of $\phi(s, N(s, B_n(s)))$, we obtain

$$\frac{d}{ds}\phi(s, N(s, B_n(s))) = 2sN(s, B_n(s)) + s^2 \frac{d}{ds}N(s, B_n(s)).$$

Evaluate the derivative at $s = 0$ gives:

$$\frac{d}{ds}\phi(0, N(0, B_n(0))) = 0,$$

which ensures that $\vartheta'(0) = \chi_1$ remains unchanged.

Hence, the general trial neural network solution for Eq. (1) will be written as

$$\hat{\chi}(s, B_n(s)) = \chi_0 + \chi_1 s + s^2 N(s, B_n(s)). \quad (24)$$

Note that, choosing $\phi(s, N(s, B_n(s)))$ in this form to ensures that the neural network approximation refines the solution while maintaining the enforced initial conditions.

4.2. The mathematical model

To construct the model, we substitute the BernsteinNN solution mentioned in Eq. (24) into Eq. (1), we obtain

$${}^c D_{0+}^{\alpha(s)} \hat{\chi}(s, B_n(s)) = \varphi(s) + \rho \int_0^s \int_0^C \mathcal{K}(x, v) \mathcal{H}(\hat{\chi}(v, B_n(v))) dv dx, \quad (25)$$

with conditions $\hat{\chi}(0, B_n(s)) = \hat{\chi}_0$, and $\hat{\chi}'(0, B_n(s)) = \hat{\chi}_1$.

The error function $E(s, B_n(s))$ is computed as

$$\begin{aligned} E(s, B_n(s)) = & \left({}^c D_{0+}^{\alpha(s)} \hat{\chi}(s, B_n(s)) - \varphi(s) - \rho \int_0^s \int_0^C \mathcal{K}(x, v) \mathcal{H}(\hat{\chi}(v, B_n(v))) dv dx \right) \\ & + \left(\hat{\chi}(0, B_n(s)) - \hat{\chi}_0 \right) + \left(\hat{\chi}'(0, B_n(s)) - \hat{\chi}_1 \right) + \lambda L2, \end{aligned} \quad (26)$$

which includes the error function from the main equation, the error from the initial conditions, and an added regularization term to ensure the stability of training process and to overcome the fitting problems and hyper-parameter λ . The regularization term $L2$ is the sum of the squared values of the weights Neural Network defined by $L2 = \sum_{i=1}^n \sum_{j=1}^{m_i} w_{ij}^2$, where n is the number

of layers in the model, m_i is the number of parameters (weights) in the i -th layer, w_{ij} represents the j -th weight in the i -th layer, w_{ij}^2 represents the square of the weight. We choose the hyper-parameter $\lambda = 10^{-4}$ to control the regularization strength.

Note that all external settings of neural network, such as the number of hidden layers, hidden units per layer, learning rate, $L2$ regularization, the regularization coefficient λ , batch size, and number of epochs, which are set before the the training process to evaluate the model's performance, are called hyper-parameters.

Moreover, the fractional derivative in Eq. (26) is computed using the definition of the Caputo derivative from Theorem 2.2, where $1 < \alpha \leq 2$, and is approximated using the trapezoidal rule in Python.

Then, the model performance is computed using the mean square error (MSE) as follows

$$\text{MSE} = \frac{1}{n} \sum_{i=0}^n E(s, B_n(s)). \quad (27)$$

Figure 1 hows the procedure for applying Bernstein neural network on our model, and Algorithm 1 demonstrates the Bernstein neural network method.

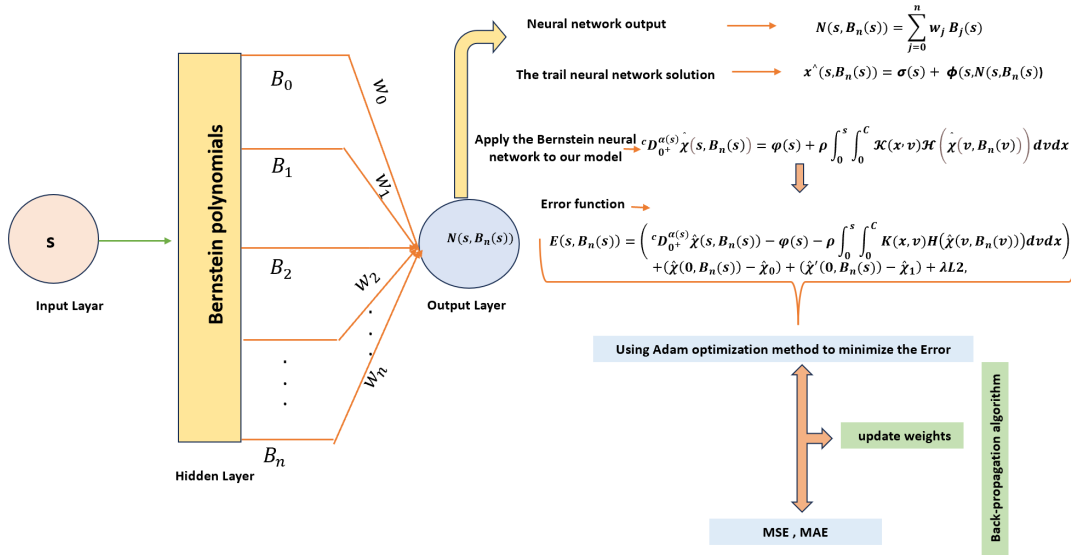


Figure 1: BernsteinNN structure for solving FVFIDEs

4.3. Update the weights

The gradient of the error function with respect to the network's weights is evaluated using back-propagation learning algorithm. Let $\zeta = [w^{[1]}, w^{[2]}, \dots, w^{[n]}]$ denotes for all wights are used in the neural network. Then, by using the chain rule, we have

$$\frac{\partial E}{\partial \zeta} = \sum_{i=0}^n \left(\frac{\partial E}{\partial B_n} \cdot \frac{\partial B_n}{\partial \zeta} \right) + 2\lambda \sum_{i=1}^n \sum_{j=1}^{m_i} w_{ij}.$$

Hence, the weight update occurs based on the computed gradients and using the Adam

Algorithm 1 Bernstein Neural Network for solving FVFIDEs

Require: Degree of Bernstein polynomial n , Number of hidden units N , Learning rate lr , Number of epochs e , the fractional degree α .

Ensure: Predicted solutions, MAE, and MSE.

- 1: Initialize model with polynomials.
- 2: Initialize optimizer and learning rate.
- 3: **for** $epoch = 1$ to e **do**
- 4: Zero the parameter gradients
- 5: Compute the loss (or the error):
- 6: Define trial solution incorporating initial boundary conditions.
- 7: Compute: the integer order derivative, the fractional derivative using Caputo derivative, the Riemann-Liouville fractional integrals.
- 8: Define the require equation which we want to solve it using the polynomial neural network.
- 9: Compute the loss(or the error) function including initial boundary conditions and $L2$ regularization.
- 10: Back-propagate the loss and update model parameters using Adam optimization method Algorithm 2.
- 11: Step the learning rate.
- 12: **end for**
- 13: **for** each value in α **do**.
- 14: Initialize model and train as described above.
- 15: Test the model at specific points s .
- 16: Compute predicted solutions and exact solution.
- 17: Calculate Mean Absolute Error (MAE) and Mean Squared Error (MSE).
- 18: Print results and plot solutions.
- 19: **end for**
- 20: Compute Errors:
- 21: MAE, MSE, then print and plot the results.

optimization method explained in Algorithm 2, where the estimates: m_t is for first moment and v_t is for second moment of the gradients, which are initialized at the initial time steps as zero vectors. β_1 and β_2 are the decay rates close to 1. The method is implemented using Python program to obtain the numerical results.

5. Numerical Example

In this section, we use the BernsteinNN approach to solve the following example with the variable order $\alpha(s) \in [1, 2]$, then we compare the results with exact solution computed at $\alpha = 2$, to ensure that the approximate solution for the variable order in that interval will be approach and converge to exact solution.

Consider the following non-linear \mathcal{VO} -FVFIDEs:

$$\begin{cases} {}^c D_{0+}^{\alpha(s)} \chi(s) = -\frac{25}{504}s^2 + \frac{749}{360}s + \int_0^s \int_0^1 (x-v)(\chi(v))^2 - \chi(v) dv dx, \\ \chi(0) = 1, \quad \chi'(0) = 0, \quad 1 < \alpha(s) \leq 2, \quad s \in [0, 1] \end{cases} \quad (28)$$

Exact solution is $\chi(s) = \frac{1}{3}s^3 + 1$ (for constant order).

Let $s = \min(s, s_k)$ on sub-interval $[s_{k-1}, s_k]$, so for this partition, the constant fractional

Algorithm 2 Adaptive Moment Estimation Method

Input: Initialize parameters $\zeta = [w^{[1]}, w^{[2]}, \dots, w^{[n]}]$, learning rate η , decay rates $\beta_1, \beta_2, \epsilon$.
Output: Updated neural network parameters ζ .
Initialize: Parameters ζ , first moment $m_t \leftarrow 0$, second moment $v_t \leftarrow 0$.
for $l = 1$ to L **do**
 Compute gradient $\frac{\partial E}{\partial \zeta^l}$.
 Update $m_t^l \leftarrow \beta_1 m_t^{l-1} + (1 - \beta_1) \frac{\partial E}{\partial \zeta^l}$.
 Update $v_t^l \leftarrow \beta_2 v_t^{l-1} + (1 - \beta_2) \left(\frac{\partial E}{\partial \zeta^l} \right)^2$.
 Compute $\hat{m}_t^l \leftarrow \frac{m_t^l}{1 - \beta_1}$.
 Compute $\hat{v}_t^l \leftarrow \frac{v_t^l}{1 - \beta_2}$.
 Update $\zeta^{l+1} \leftarrow \zeta^l - \frac{\eta}{\sqrt{\hat{v}_t^l + \epsilon}} \hat{m}_t^l$.
end for
return ζ .

order equation

$$\begin{cases} {}^c D_{0+}^{\alpha_k} \chi(s) = -\frac{25}{504} s^2 + \frac{749}{360} s + \int_{s_{k-1}}^s \int_0^1 (x-v)(\chi(v))^2 - \chi(v) dv dx, \\ \chi(s_{k-1}) = 1, \quad \chi'(s_{k-1}) = 0, \quad s \in J_k \end{cases} \quad (29)$$

has at least one solution by using Theorem 3.2, since the continuous functions \mathcal{H}, φ and \mathcal{K} satisfy the conditions (A1)-(A3), such that $L = 1$, $\mathcal{K}^* = 1$, $\|\varphi\| = 2.13016$, and $\mathcal{H}(\chi(s))$ is bounded on j_k with $z = 2$. Hence Eq. (28) has at least one solution. Moreover, the above equation has a unique solution and satisfies Theorem 3.3, since for each value of $\alpha_k \in (1, 2]$, there exist a constant $\mathcal{R} \in [0.166667, 0.5]$, and hence Eq. (28) has a unique solution.

The trial neural network solution $\hat{\chi}(s, B_n(s))$ can be chosen as

$$\hat{\chi}(s, B_n(s)) = 1 + s^2 N(s, B_n(s)), \quad (30)$$

and satisfy the initial conditions in Eq. (28).

Substitute the trial neural network solution Eq. (30) into Eq. (28), we obtain

$$\begin{aligned} & {}^c D_{0+}^{\alpha(s_i)} \hat{\chi}(s_i, B_n(s_i)) \\ &= -\frac{25}{504} s_i^2 + \frac{749}{360} s_i + \int_0^{s_i} \int_0^1 (x-v)[(\hat{\chi}(v, B_n(v)))^2 - \hat{\chi}(v, B_n(v))] dv dx, \end{aligned} \quad (31)$$

with conditions $\hat{\chi}(0, B_n(s_i)) = 1$, and $\hat{\chi}'(0, B_n(s_i)) = 0$, where s_i are the collocation points.

The error function computed as

$$\begin{aligned} \text{MSE} = & \frac{1}{N} \sum_{i=1}^N \left({}^c D_{0+}^{\alpha(s_i)} \hat{\chi}(s_i, B_n(s_i)) + \frac{25}{504} s_i^2 - \frac{749}{360} s_i \right. \\ & \left. - \int_0^{s_i} \int_0^1 (x-v) (\hat{\chi}^2(v, B_n(v)) \hat{\chi}(v, B_n(v))) dv dx \right)^2 + \lambda L2, \end{aligned} \quad (32)$$

where $L2 = \sum_{i=1}^n \sum_{j=1}^{m_i} w_{ij}^2$, number of epochs = 300, number of collocation points equal

11. For the integral sign, we use the trapezoidal rule. Then, we train the BernsteinNN by minimizing the error function in Eq. (32) using Adam optimizer Algorithm 2. During training, the weights w_k will be adjusted to reduce the residuals of the FVFIDEs and satisfy the initial conditions.

Since hyper-parameters such as the degree of Bernstein polynomials, learning rate and λ significantly affect the accuracy and convergence of the neural network solution, we aimed to select suitable values that satisfy our goals. To achieve this, multiple values of Bernstein polynomial degree, learning rate and λ were tested during the training process. The accuracy of the predicted solution was evaluated using the Mean Squared Error (MSE). The results showed that increasing N improved the approximation accuracy but also increased the computational cost and risk of over-fitting. At this point, the role of $L2$ regularization became essential to overcoming of over-fitting issues, and ensuring a more stable solution.

The optimal choice, $N = 35$, was selected as it provided a good balance between accuracy and computational efficiency, yielding minimal error with $\lambda = 10^{-4}$. Similarly, after testing different learning rates, we found that when the learning rate was set to 10^{-3} , the solution remained stable and convergent. These parameters were applied across different values of $\alpha(s)$. We choose the variable order such that satisfy $\forall s \in [0, 1], \alpha(s) \in [1, 2]$, as follow:

$$\begin{aligned}\alpha_1(s) &= 1 + \frac{\log(1+s)}{\log(2)}, \\ \alpha_2(s) &= 1 + \frac{\exp(s) - 1}{e - 1}, \\ \alpha_3(s) &= s^5 + 1, \\ \alpha_4(s) &= s^2 + 1, \\ \alpha_5(s) &= s + 1, \\ \alpha_6(s) &= s^8 + 1, \\ \alpha_7(s) &= 2.\end{aligned}$$

Table 1 shows the comparison between the exact solution for the constant order $\alpha = 2$ and the approximate solutions for different values of the variable order. The parameters used are $N = 35$, number of epochs = 300, and a learning rate 10^{-3} . The results confirm the efficiency of the BernsteinNN method, particularly when compared to the approximate solution at $\alpha_7 = 2$, which shows a high degree of convergence. This indicates that the method can also be effectively applied to constant fractional-order problems, yielding accurate approximations with reduced computational effort. Additionally, when testing different variable order functions $\alpha(s)$, we observe that at $\alpha_3(s)$ and $\alpha_5(s)$, the results converge to exact solution.

Table 2 further supports this by showing that the Mean Squared Error (MSE) values reflect the efficiency of the BernsteinNN method in solving \mathcal{VO} problems, achieving a minimal error of 10^{-4} .

Figures 2 and 3 show the comparison between exact and approximate solution with degree $N = 35$ and epochs 300 at different values of variable orders. Figure 4 demonstrate that the approximate solution and the error functions are converges to the exact.

6. Conclusion

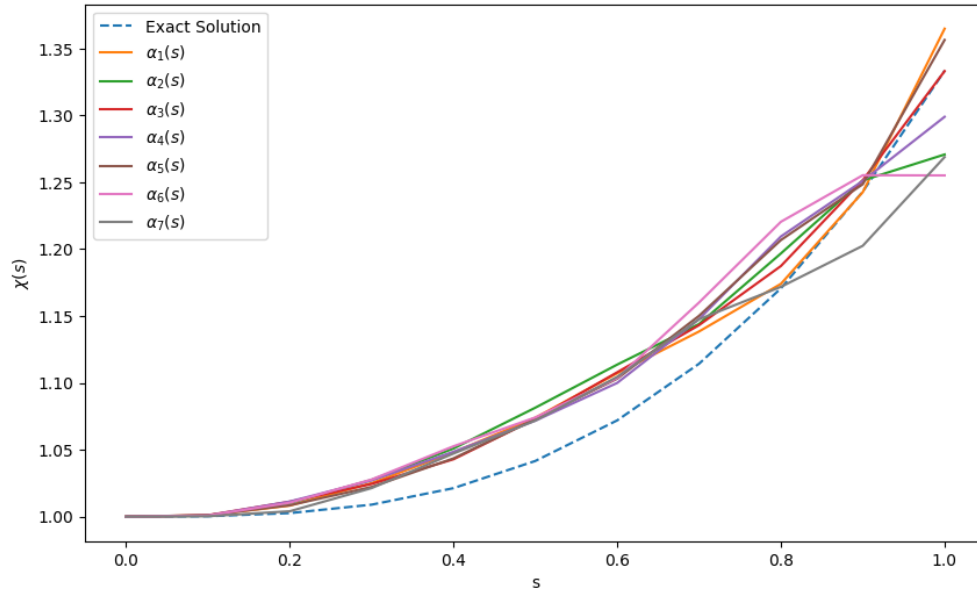
In this paper, we investigated the existence and uniqueness of the solution for \mathcal{VO} fractional Volterra-Fredholm integro-differential equations (FMVFIDEs) in Caputo sense, under the boundedness and lipschitz continuity conditions. The \mathcal{VO} function was divided into piecewise constant functions using uniformly partitions. By employing fixed-point theorems, we rigorously verified the existence and uniqueness of the solution. To obtain an approximate solution, we

Table 1: The approximate solution of BernsteinNN at different values of $\alpha(s)$.

| s | Exact Solution | Approximate solution | | | | | | |
|-----|----------------|----------------------|---------------|---------------|---------------|---------------|---------------|---------------|
| | | $\alpha_1(s)$ | $\alpha_2(s)$ | $\alpha_3(s)$ | $\alpha_4(s)$ | $\alpha_5(s)$ | $\alpha_6(s)$ | $\alpha_7(s)$ |
| 0.1 | 1.000333 | 1.000568 | 1.001174 | 1.000862 | 1.001541 | 1.000914 | 1.001352 | 1.000368 |
| 0.2 | 1.002667 | 1.007848 | 1.010922 | 1.010943 | 1.012725 | 1.008914 | 1.012886 | 1.004608 |
| 0.3 | 1.009000 | 1.022025 | 1.024880 | 1.027304 | 1.028278 | 1.023596 | 1.028451 | 1.024173 |
| 0.4 | 1.021333 | 1.042530 | 1.044584 | 1.045774 | 1.048540 | 1.043854 | 1.049054 | 1.051452 |
| 0.5 | 1.041667 | 1.078022 | 1.070922 | 1.068858 | 1.070879 | 1.075612 | 1.079194 | 1.079534 |
| 0.6 | 1.072000 | 1.121331 | 1.102906 | 1.106854 | 1.093101 | 1.119202 | 1.105836 | 1.106992 |
| 0.7 | 1.114333 | 1.155482 | 1.137042 | 1.146840 | 1.130736 | 1.158764 | 1.126525 | 1.138054 |
| 0.8 | 1.170667 | 1.191375 | 1.191747 | 1.183194 | 1.180272 | 1.211122 | 1.184094 | 1.179724 |
| 0.9 | 1.243000 | 1.257099 | 1.255044 | 1.233893 | 1.266549 | 1.252740 | 1.246995 | 1.258398 |
| 1.0 | 1.333333 | 1.379210 | 1.210313 | 1.376331 | 1.296375 | 1.364396 | 1.233887 | 1.371307 |

Table 2: The MSE of BernsteinNN for different values of $\alpha(s)$.

| | $\alpha_1(s)$ | $\alpha_2(s)$ | $\alpha_3(s)$ | $\alpha_4(s)$ | $\alpha_5(s)$ | $\alpha_6(s)$ | $\alpha_7(s)$ |
|-----|-----------------------|------------------------|-----------------------|-----------------------|-----------------------|------------------------|-----------------------|
| MSE | 8.02×10^{-4} | 1.719×10^{-3} | 5.55×10^{-4} | 4.36×10^{-4} | 8.01×10^{-4} | 1.276×10^{-3} | 5.57×10^{-4} |

Figure 2: Comparison between exact and approximate solution of BernsteinNN with degree $N = 35$ for different variable order after 300 epochs.

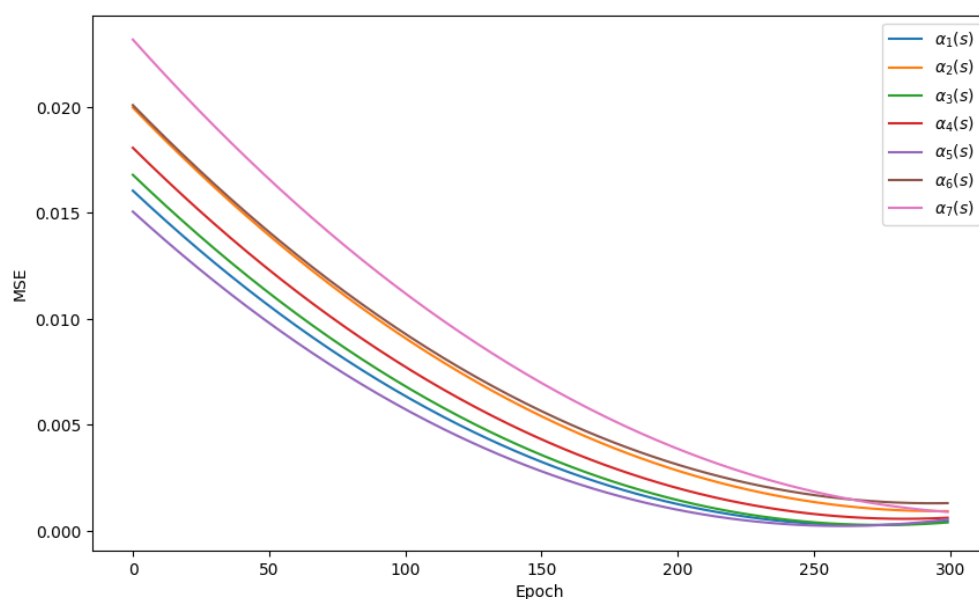


Figure 3: MSE of BernsteinNN for different variable order.

proposed the Bernstein Neural Network (BernsteinNN) method for solving \mathcal{VO} Caputo FV-FIDEs. A numerical example was presented to illustrate the effectiveness and accuracy of the proposed approach. The results showed that BernsteinNN provides highly accurate approximations, making it a promising method for solving \mathcal{VO} fractional problems. Future work will focus on extending this approach to more complex fractional integro-differential equations, including multi-term fractional models. Improving the optimization techniques for used in training the neural network will also be considered when studying \mathcal{VO} functions. Moreover, applying the proposed method to real-world problems will be considered for further study.

References

- Agarwal P., El-Sayed A.A. & Tariboon J. 2021. Vieta-Fibonacci operational matrices for spectral solutions of variable order fractional integro-differential equations. *Journal of Computational and Applied Mathematics* **382**: 113063.
- Ahmed K.I.A., Adam H.D.S., Almutairi N. & Saber S. 2024. Analytical solutions for a class of variable-order fractional Liu system under time-dependent variable coefficients. *Results in Physics* **56**: 107311.
- Albasheir N.A., Alsinai A., Niazi A.U.K., Shafqat R., Romana, Alhagyan M. & Gargouri A. 2023. A theoretical investigation of Caputo variable order fractional differential equations: existence, uniqueness, and stability analysis. *Computational and Applied Mathematics* **42**(8): 367.
- Alharthi N.H., Atangana A. & Alkahtani B.S. 2023. Study of a cauchy problem of fractional order derivative with variable order fractal dimension. *Results in Physics* **49**: 106524.
- Alsa'di K., Nik Long N.M.A. & Eshkuvatov Z.K. 2024. Theoretical and numerical studies of fractional volterra-fredholm integro-differential equations in Banach space. *Malaysian Journal of Mathematical Sciences* **18**(3).
- Awad Y., Fakhri H. & Alkhezi Y. 2023. Existence and uniqueness of variable-order φ -Caputo fractional two-point nonlinear boundary value problem in Banach algebra. *Axioms* **12**(10): 935.
- Babaei A., Jafari H. & Banihashemi S. 2020. Numerical solution of variable order fractional nonlinear quadratic integro-differential equations based on the sixth-kind Chebyshev collocation method. *Journal of Computational and Applied Mathematics* **377**: 112908.
- Benkerrouche A., Etemad S., Souid M.S., Rezapour S., Ahmad H. & Botmart T. 2023. Fractional variable order differential equations with impulses: A study on the stability and existence properties. *AIMS Mathematics* **8**(1): 775–791.

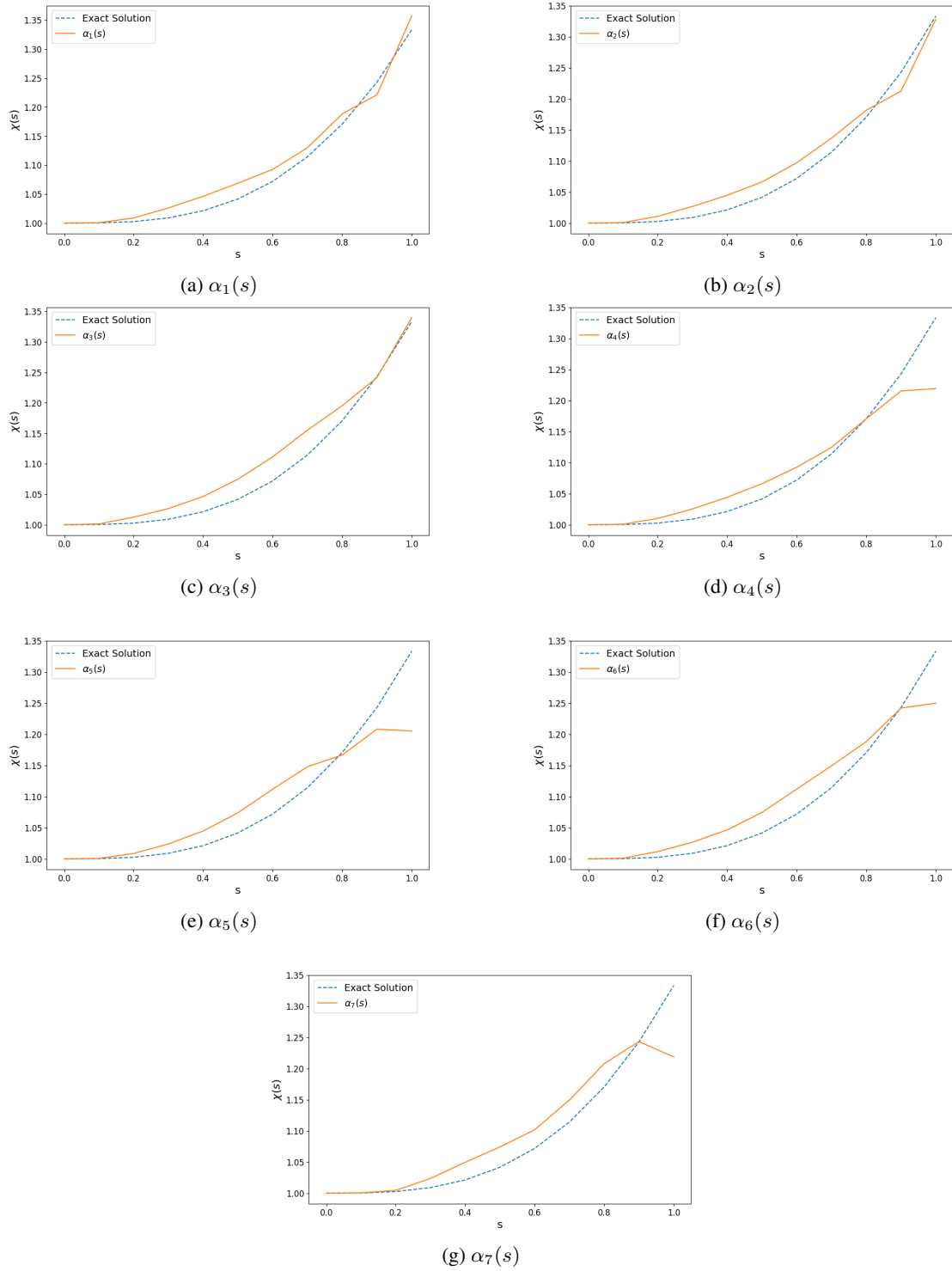


Figure 4: Exact and approximate solutions for different variable order functions after 300 epochs.

- Benkerrouche A., Souid M.S., Jarad F. & Hakem A. 2022. On boundary value problems of Caputo fractional differential equation of variable order via Kuratowski MNC technique. *Advances in Continuous and Discrete Models* **2022**(1): 43.
- Bhrawy A.H. & Zaky M.A. 2016. Numerical algorithm for the variable-order Caputo fractional functional differential equation. *Nonlinear Dynamics* **85**: 1815–1823.
- Bouazza Z., Souhila S., Etemad S., Souid M.S., Akgül A., Rezapour S. & De la Sen M. 2023a. On the Caputo-Hadamard fractional IVP with variable order using the upper-lower solutions technique. *AIMS Math* **8**(3): 5484–5501.
- Bouazza Z., Souid M.S., Hussin C.H.C., Mandangan A. & Sabit S. 2023b. Variable-order implicit fractional differential equations based on the kuratowski mnc technique. *Malaysian Journal of Mathematical Sciences* **17**(3): 305–332.
- Cao J. & Qiu Y. 2016. A high order numerical scheme for variable order fractional ordinary differential equation. *Applied Mathematics Letters* **61**: 88–94.
- Derakhshan M.H. 2022. Existence, uniqueness, Ulam-Hyers stability and numerical simulation of solutions for variable order fractional differential equations in fluid mechanics. *Journal of Applied Mathematics and Computing* **68**(1): 403–429.
- Ganji R.M., Jafari H. & Nemati S. 2020. A new approach for solving integro-differential equations of variable order. *Journal of Computational and Applied Mathematics* **379**: 112946.
- Heydari M.H. & Atangana A. 2020. An optimization method based on the generalized Lucas polynomials for variable order space-time fractional mobile-immobile advection-dispersion equation involving derivatives with non-singular kernels. *Chaos, Solitons & Fractals* **132**: 109588.
- Kachia K., Solís-Pérez J.E. & Gómez-Aguilar J.F. 2020. Chaos in a three-cell population cancer model with variable order fractional derivative with power, exponential and Mittag-Leffler memories. *Chaos, Solitons & Fractals* **140**: 110177.
- Kilbas Anatoliĭ A., Srivastava H.M. & Trujillo J.J. 2006. *Theory and Applications of Fractional Differential Equations (Vol. 204)*. Amsterdam, NL: Elsevier.
- Kilbas A.A. 2001. Hadamard-type fractional calculus. *J. Korean Math. Soc* **38**(6): 1191–1204.
- Li X., Li H. & Wu B. 2017. A new numerical method for variable order fractional functional differential equations. *Applied Mathematics Letters* **68**: 80–86.
- Malesza W., Macias M. & Sierociuk D. 2019. Analytical solution of fractional variable order differential equations. *Journal of Computational and Applied Mathematics* **348**: 214–236.
- Moghadam A.S., Arabameri M., Barfeie M. & Baleanu D. 2020. Numerical solution of space-time variable fractional order advection-dispersion equation using jacobi spectral collocation method. *Malaysian Journal of Mathematical Sciences* **14**(1): 139–168.
- Moghaddam B.P. & Machado J.A.T. 2017. A stable three-level explicit spline finite difference scheme for a class of nonlinear time variable order fractional partial differential equations. *Computers & Mathematics with Applications* **73**(6): 1262–1269.
- Rezapour S., Souid M.S., Bouazza Z., Hussain A. & Etemad S. 2022. On the fractional variable order thermostat model: Existence theory on cones via piece-wise constant functions. *Journal of Function Spaces* **2022**: 8053620.
- Samko S.G. 1995. Fractional integration and differentiation of variable order. *Analysis Mathematica* **21**(3): 213–236.
- Sarwar S. 2022. On the existence and stability of variable order Caputo type fractional differential equations. *Fractal and Fractional* **6**(2): 51.
- Tavares D., Almeida R. & Torres D.F.M. 2016. Caputo derivatives of fractional variable order: Numerical approximations. *Communications in Nonlinear Science and Numerical Simulation* **35**: 69–87.
- Van Bockstal K., Zaky M.A. & Hendy A.S. 2022. On the existence and uniqueness of solutions to a nonlinear variable order time-fractional reaction-diffusion equation with delay. *Communications in Nonlinear Science and Numerical Simulation* **115**: 106755.
- Xu Y., Telli B., Souid M.S., Etemad S., Xu J. & Rezapour S. 2024. Stability on a boundary problem with RL-Fractional derivative in the sense of Atangana-Baleanu of variable-order. *Electronic Research Archive* **32**(1): 134–159.
- Yuan W., Liang H. & Chen Y. 2023. On the convergence of piecewise polynomial collocation methods for variable-order space-fractional diffusion equations. *Mathematics and Computers in Simulation* **209**: 102–117.
- Zheng X. 2022. Numerical approximation for a nonlinear variable order fractional differential equation via a collo-

- cation method. *Mathematics and Computers in Simulation* **195**: 107–118.
- Zhou Y. 2023. *Basic Theory of Fractional Differential Equations*. 3rd Ed. Singapore: World Scientific Publishing Company.
- Zhou Y., Wang J. & Zhang L. 2016. *Basic Theory Of Fractional Differential Equations*. 2nd Ed. Singapore: World Scientific.
- Zuniga-Aguilar C.J., Gómez-Aguilar J.F., Escobar-Jiménez R.F. & Romero-Ugalde H.M. 2019. A novel method to solve variable order fractional delay differential equations based in lagrange interpolations. *Chaos, Solitons & Fractals* **126**: 266–282.
- Zúñiga-Aguilar C.J., Romero-Ugalde H.M., Gómez-Aguilar J.F., Escobar-Jiménez R.F. & Valtierra-Rodríguez M. 2017. Solving fractional differential equations of variable order involving operators with Mittag-Leffler kernel using artificial neural networks. *Chaos, Solitons & Fractals* **103**: 382–403.

Department of Mathematics and Statistics
Faculty of Science
Universiti Putra Malaysia
43400 UPM Serdang
Selangor, MALAYSIA
E-mail: kawther.alsaadi@yahoo.com , nmasri@upm.edu.my*

Received: 4 February 2025
Accepted: 4 May 2025

*Corresponding author